Available online at www.sciencedirect.com
ScienceDirect
IFAC PapersOnLine 59-20 (2025) 970–975

Large-Scale Planetary Exploration and Monitoring in a Prior Unknown Environment Using Multi-Rover System

Yuxuan Hu * **Liang Zhang** * **Kangwen Lin** *

* *the School of Electrical Engineering and Automation, Anhui University, Hefei 230093, China.(e-mail: liangzhang@ahu.edu.cn).*

Abstract:
Multi-rover systems are increasingly vital for planetary exploration due to their efficiency and robustness. As the complexity of exploration missions increases, a key challenge is how to deploy rovers in unknown environments for efficient coverage and monitoring. To solve this problem, this paper proposes a distributive and online estimation framework and a correspondingly coverage control strategy. The proposed estimation framework can estimate an unknown environment using a probabilistic and non-parametric method, with the coverage control strategy driving each rover to the optimal position. Finally, the performance of this estimation framework and its coverage control strategy is verified through a large number of simulation results.

Keywords: Multi-rover system, Unknown environment, estimation framework, Coverage control strategy

1. INTRODUCTION

In recent years, with the increasing complexity of planetary exploration missions, rovers face more stringent technical requirements in terms of size, performance, and energy consumption. The Multi-Rover System (MRS) composed of multiple rovers has become the preferred solution for planetary exploration, especially large-scale monitoring missions, due to its strong adaptability, high processing efficiency and robustness Dengyun et al. (2016). Coverage control, as a key technology to achieve efficient and comprehensive coverage, is an important part of MRS control. Moreover, coverage control algorithms are widely used in various key tasks, such as target monitoring Gu et al. (2018), terrain coverage Xu et al. (2011), positioning services Zhang et al. (2021) and communication services Arum et al. (2020), and have important engineering application value. In coverage missions, MRS acts as distributed coverage units, with target distribution represented by its density function. The control objective is to dynamically optimize deployment based on spatial density distribution, enabling precise coverage and prioritized monitoring of high-density regions.

Therefore, in order to efficiently obtain high-value information, large-scale exploration and monitoring missions require driving MRS to achieve optimal coverage of unknown planetary regions. However, it should be noted that planetary exploration often involves areas that humans have never set foot on. In addition, due to multiple factors such as cosmic radiation interference, extreme environment of outer space, and bandwidth limitations of long-distance communications WANG et al. (2022); Kisantal et al. (2020), it is difficult to obtain high-precision terrain prior information in the mission space. This environment, where prior information is completely unknown, poses a significant challenge to developing coverage deployment strategies for MRS.

Research in the field of coverage control mainly focuses on the optimization of control strategies under known environmental density Cortes et al. (2004); Zhong and Cassandras (2011). For example, in algorithms, Yu et al. (2021) introduced a K-means clustering dynamic coverage planner, overcoming traditional object coverage constraints. It guides intelligent units to optimal positions via discrete sliding mode control. For energy efficiency, Wang et al. (2018) proposed a particle swarm optimization coverage algorithm, enhancing coverage while lowering energy use in sensor networks. In unknown density fields, current approaches usually estimate the density function and then design coverage strategy accordingly. Demetriou and Hussein (2009); Carron et al. (2015). For example, Schwager et al. (2009) developed a decentralized approach using Gaussian basis functions to estimate weight parameters online, enabling density estimation and optimal coverage. Based on this, Gong et al. (2024) proposed an adaptive control algorithm employing Gaussian approximation for wind field estimation and airship control. Similarly, Popović et al. (2020) introduced a general centralized framework for density field reconstruction and path planning.

Although important progress has been made in the coverage control problem under unknown density information, traditional methods often have certain assumptions and restrictions on the unknown density prior or have a relatively complex estimation process, or use centralized estimation methods. Therefore, we propose a distributive and online estimation framework under unknown planetary environment and a coverage strategy based on this framework. The proposed framework can estimate the density field

10.1016/j.ifacol.2025.11.279

distribution trend without prior information. And the strategy can drive the rovers to near-optimal positions. Its estimation complexity depends only on map resolution and can be adaptively adjusted according to practical needs during exploration.

The core contributions of this work are:

(1) A distributive and online estimation framework, including data collection, iterative estimation and data fusion. It models and estimates a priori completely unknown environment in probabilistic and non-parametric ways.
(2) A coverage strategy based on this estimation framework, drives the MRS from an arbitrary initial position to a nearly optimal coverage position.
(3) Extensive simulation results verify the effectiveness and robustness of the proposed estimation framework and coverage control strategy.

2. PROBLEM FORMULATION

In planetary exploration missions, considering the coverage and monitoring challenges for an unknown mission space $\boldsymbol{T} \subset \mathbb{R}^2$ on planetary surfaces using a MRS comprising n rovers. The position of the i-th rover within region $\boldsymbol{T}$ is defined as $p_i = (x_i, y_i)$. Coverage control in MRS typically involves achieving complete coverage by optimizing the spatial distribution of the rover position set $\boldsymbol{P} = \{p_1, p_2, \cdots, p_n\}$.

Classical coverage control research is usually carried out under the premise that the target density distribution is known a priori. A typical solution under this condition is coverage control based on Voronoi segmentation,such as Schwager et al. (2009), Cortes et al. (2004). The core idea involves partitioning the mission space $\boldsymbol{T}$ among rovers through Voronoi segmentation, thus decomposing the global problem into local optimization problems in each Voronoi area. Specifically, for a convex and bounded mission space $\boldsymbol{T}$, the Voronoi segmentation $\boldsymbol{V} = \{\boldsymbol{V}_1, \boldsymbol{V}_2, \cdots, \boldsymbol{V}_n\}$ can be defined as

$$\boldsymbol{V}_i = \{q \in \boldsymbol{T} \mid \|q - p_i\| \le \|q - p_j\|, \forall j \ne i\} \tag{1}$$

Note that the Voronoi region of i-th rover V_i can be interpreted as the set of points q closest to rover p_i in mission space $\boldsymbol{T}$. To quantitatively evaluate the coverage performance of the MRS over the mission space $\boldsymbol{T}$, the coverage cost function is defined as

$$\boldsymbol{C} = \sum_{i=1}^{n} \int_{V_i} f(\|q - p_i\|)\phi(q)\, dq \tag{2}$$

Let $\|\cdot\|$ represent the Euclidean distance. Define the function $f(\|q - pi\|) = \|q - pi\|^2, f(\|q - pi\|) \in \mathbb{R}^+$ to characterize the coverage quality loss of rover p_i at position q. Specifically, the farther away from the rover p_i, the less reliable the measurements. $\phi(q) \in \mathbb{R}^+$ is the density function in mission space $\boldsymbol{T}$ (for example, the terrain distribution or mineral resource distribution), reflecting the probability of an event occurring at q.

Therefore, in order to obtain better coverage, we should try to reduce coverage quality loss as much as possible. The optimal coverage problem for region $\boldsymbol{T}$ is translated into minimizing the cost function $\boldsymbol{C}$ by optimizing the spatial distribution of each rover. According to Du et al. (1999), the standard solution to the optimization problem can be obtained through calculations as

$$\frac{\partial \boldsymbol{C}}{\partial p_i} = -2 \int_{V_i} (q - p_i)\phi(q) dq = -2M_{V_i}(C_{V_i} - p_i) \tag{3}$$

where M_{V_i} represents the mass of V_i and C_{V_i} represents its centroid. When the rover position $p_i = C_{V_i}$, the cost function $\boldsymbol{C}$ reaches its extreme value. This shows that the optimal coverage based on Voronoi segmentation is essentially achieved by moving the rover p_i to the centroid of its Voronoi region $\boldsymbol{V}_i$.

However, in planetary exploration, factors such as cosmic radiation interference make it difficult to obtain prior information about the environment. Therefore, for coverage tasks in such scenarios, it is necessary to first establish an estimation model for the unknown density field. So the function $\boldsymbol{C}$ needs to be transformed into the following form

$$\boldsymbol{C} = \sum_{i=1}^{n} \int_{V_i} \|q - p_i\|^2 \hat{\phi}(q)\, dq \tag{4}$$

where $\hat{\phi}(q) \in \mathbb{R}^+$ is the estimated distribution of the density function $\phi(q)$. Overall, coverage and monitoring tasks in a priori unknown environments can be transformed into the following core problems:

Problem 1. How to implement a distributive and online estimation $\hat{\phi}(q)$ of the density function $\phi(q)$ in the unknown mission space $\boldsymbol{T}$ using local measurements and communication, and then achieve optimal monitoring of the entire space $\boldsymbol{T}$ by minimizing the cost function $\boldsymbol{C}$

3. SYSTEM FRAMEWORK

In order to achieve coverage control of the unknown density field area, we propose the whole framework including density estimation and coverage control as shown in Fig. 1. They are explained in detail in the next three subsections.

3.1 Region division

To estimate an unknown density field, a MRS must conduct multiple sampling operations within mission space $\boldsymbol{T}$ to acquire sufficient modeling data. This requires coordinated rover path planning and sampling strategies. We propose a Voronoi-based spatial planning method to optimize MRS deployment for assigning sampling regions. The method guides each rover from any initial position to its corresponding Voronoi subregion, improving sampling efficiency while preventing collisions through constrained operational boundaries. During deployment, the global cost function is defined according to formula (2) as follows:

$$\boldsymbol{C}_0 = \sum_{i=1}^{n} \int_{V_i} \|q - p_i\|^2 \phi_0(q) dq \tag{5}$$

The density function $\phi_0(q)$ is set to be uniformly distributed. At this time, (3) indicates that each rover converges to its Voronoi region's centroid C_{V_i}. In particular, when the density function is uniformly distributed, the centroid C_{V_i} degenerates into the geometric centroid, and the Voronoi regions of each rover tend to be uniform

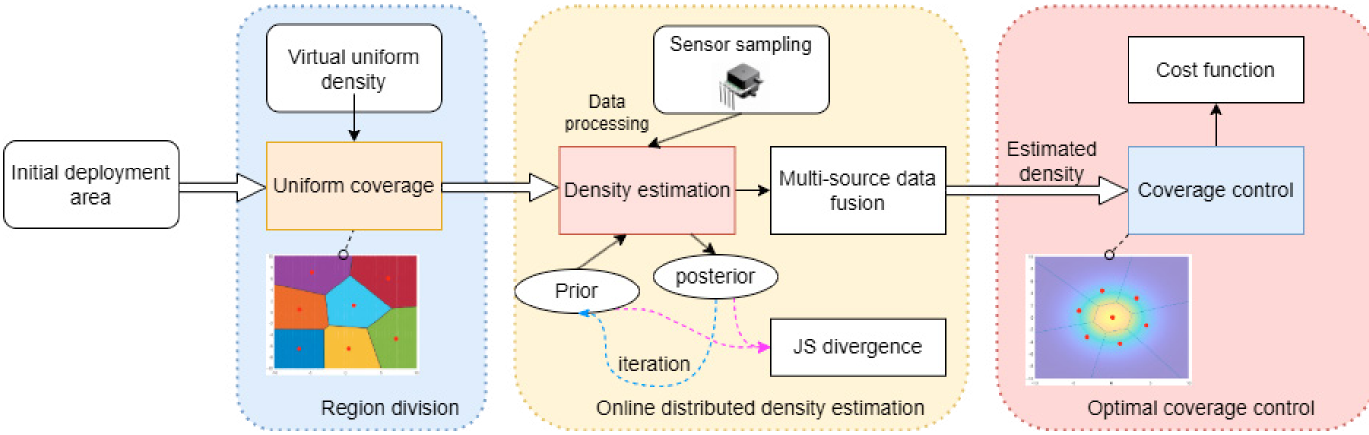

Fig. 1. Overall framework. The framework mainly consists of three modules: First, mission space $\boldsymbol{T}$ is divided into regions. Then, a probability estimation and mapping model of the unknown density field is established. Finally, the optimal coverage control of the space $\boldsymbol{T}$ based on the weighted estimated density is achieved.

area division. Based on this, by dynamically updating the Voronoi segmentation layout in the mission space $\boldsymbol{T}$ and continuously driving the rovers to converge to their respective Voronoi centroids, a balanced distribution of rovers in the mission space can be achieved. This establishes the foundation for subsequent density estimation.

3.2 Density mapping

To achieve efficient estimation of unknown density fields, this subsection proposes a collaborative estimation framework that combines sampling and distributed and online Gaussian Process (GP) regression. Combined with the sampled data set, the framework uses an online GP iteration method to continuously update the model, gradually narrowing the difference between the estimated value $\hat{\phi}(q)$ and the true density $\phi(q)$. At the same time, a multi-source fusion mechanism is introduced in the iterative process to realize data exchange and fusion between rovers, effectively improving the estimation accuracy. By establishing a quantitative index of the difference between iterations and setting a stability criterion, when the difference converges to a preset threshold, the process is judged to reach a stable state. The specific implementation details and theoretical derivation are detailed in Sect. 4

This method requires no prior assumptions about the target density function, demonstrating strong adaptability. The computational complexity for each rover depends solely on the raster map resolution, remaining constant regardless of iteration counts or swarm size.

3.3 Optimal coverage

After obtaining the estimated unknown density function set through the estimation method, we use the average density distribution of the set to construct the final estimated density. This processing helps reduce the uncertainty of single rover estimates, thereby improving accuracy. Therefore, after substituting the estimated density, we obtain the specific form of the cost function $\boldsymbol{C}$ as shown in equation (4).

By minimizing the cost function $\boldsymbol{C}$, the positions $\boldsymbol{P}^* = \{p_1^*, p_2^*, \cdots, p_n^*\}$ of MRS are dynamically adjusted to an balanced state that satisfies (3). At this time, rovers reaches the centroid of each Voronoi region weighted by the density function $\hat{\phi}(q)$, thus achieving optimal coverage of the mission space.

4. MAPPING APPROACH

In Sect. 3.2, we proposed the estimation principle of the density field estimation framework. This section will systematically introduce the implementation process.

While modeling target density distributions, GP is widely used due to its probabilistic and non-parametric characteristics Williams and Rasmussen (2006).The density function $\boldsymbol{\phi} : \phi(q) \in \mathbb{R}^+$ is modeled as:$\boldsymbol{\phi} \sim \mathcal{GP}(\boldsymbol{\mu}, \boldsymbol{\Sigma})$,where $\boldsymbol{\mu}$ is the mean function and $\boldsymbol{\Sigma}$ is the covariance matrix determined by a kernel function. According to Williams and Rasmussen (2006), the kernel function can be pre-trained using historical map data to match the characteristics of $\boldsymbol{\phi}$. In addition, we assume that observations incorporate Gaussian noise: $z_i = \phi_i + \varepsilon$, where $\varepsilon \sim N(0, \sigma_n^2)$. For unknown spaces, we assume a constant prior mean $\boldsymbol{\mu}^-$ and compute the prior covariance $\boldsymbol{\Sigma}^-$ using standard GP regression Reece and Roberts (2010):

$$\begin{aligned}\boldsymbol{\Sigma}^- &= \mathcal{K}(X^*, X^*) \\ &\quad - \mathcal{K}(X^*, X)\left[\mathcal{K}(X, X) + \sigma_n^2 I_n\right]^{-1}\mathcal{K}(X^*, X)^\top\end{aligned} \tag{6}$$

where I_n is an $n \times n$ unit matrix. Therefore, each rover builds its own prior model using its observation data.

Iteratively updating the GP's expectation and covariance parameters according to the measurement data, and driving the model to gradually converge to the true value, is the core idea of the update method proposed in the estimate framework. Given the constant prior means $\boldsymbol{\mu}^-$ and the prior covariance $\boldsymbol{\Sigma}^-$ determined by (6), a prior GP model $\hat{\boldsymbol{\phi}}^- \sim \mathcal{GP}(\boldsymbol{\mu}^-, \boldsymbol{\Sigma}^-)$ of unknown density fields can be established.

During sampling, a zigzag sampling strategy is proposed for each Voronoi region $\boldsymbol{V}_i$. First, a grid sampling point with a resolution of a_m is generated and a zigzag path is planned. During the iteration, the resolution is attenuated according to $a_{m+1} = \alpha a_m,\ (\alpha \in (0,1))$ to achieve two-stage sampling from coarse to fine and avoid repetition.Its specific effects are shown in Sect. 5.

For the rover p_i, we assume that it obtains s independent measurements $\boldsymbol{z} = \{z_1, z_2, \cdots, z_s \mid z_i \in \mathbb{R}^+\}$ from the sampling points $\boldsymbol{X} = \{X_1, X_2, \cdots, X_s \mid X_s = (x_s, y_s) \in \boldsymbol{T}\}$ during one iteration. Through the maximum a posteriori estimation method, the prior can be fused with the likelihood $\phi(\boldsymbol{z}) \sim \boldsymbol{N}(\mu_s, {\sigma_s}^2)$ composed of these measurements to obtain the posterior estimate. The Kalman Filter (KF) update equation is selected as the iterative method for posterior density estimation, and the posterior estimate obtained can be expressed as $\hat{\boldsymbol{\phi}}^+ \sim \mathcal{GP}(\boldsymbol{\mu}^+, \boldsymbol{\Sigma}^+)$. From Reece and Roberts (2010), The calculation formulas for the posterior mean $\boldsymbol{\mu}^+$ and the posterior covariance $\boldsymbol{\Sigma}^+$ are as follows

$$\boldsymbol{\mu}^+ = \boldsymbol{\mu}^- + \boldsymbol{K}\boldsymbol{e} \tag{7}$$

$$\boldsymbol{\Sigma}^+ = \boldsymbol{\Sigma}^- - \boldsymbol{K}\boldsymbol{H}\boldsymbol{\Sigma}^- \tag{8}$$

where $\boldsymbol{K} = \boldsymbol{\Sigma}^- \boldsymbol{H}^\top \boldsymbol{S}^{-1}$ is the Kalman gain, which is used to balance the weights of prediction and observation. $\boldsymbol{S} = \boldsymbol{H}\boldsymbol{\Sigma}^-\boldsymbol{H}^\top + \boldsymbol{R}$ is the covariance deviation and $\boldsymbol{e} = \boldsymbol{z} - \boldsymbol{H}\boldsymbol{\mu}^-$ represents the observation deviation. $\boldsymbol{R}$ is a $s \times s$ diagonal matrix, representing the covariance of the observation noise ε. $\boldsymbol{H}$ is an $s \times n$ observation matrix that maps the state values in the prior to the observation space. Therefore, equation (7) and (8) pass the mean and covariance in the GP model as iterative data and update them in a loop.

In the distributed estimation process, each rover generates its own estimated mapping $\hat{\boldsymbol{\phi}} = \left\{\hat{\boldsymbol{\phi}}_1, \hat{\boldsymbol{\phi}}_2, \cdots, \hat{\boldsymbol{\phi}}_n\right\}$ for the unknown density. The fusion mechanism will enable the estimated density of rover p_i to fuse the estimated results of its adjacent numbered rovers. Finally, the set of estimated distributions of MRS to the unknown density $\boldsymbol{\phi}$ can be obtained $\hat{\boldsymbol{\phi}}^* = \left\{\hat{\boldsymbol{\phi}}_1^*, \hat{\boldsymbol{\phi}}_2^*, \cdots, \hat{\boldsymbol{\phi}}_n^*\right\}$.

During estimation, the deviation between iterations serves as a convergence criterion during online estimation. We employ Jensen–Shannon (JS) divergence, an improved version of Kullback-Leibler (KL) divergence, to measure differences between distributions:

$$JSD(P \parallel Q) = \frac{1}{2} KL\left(P \parallel M\right) + \frac{1}{2} KL\left(Q \parallel M\right) \tag{9}$$

where $M = \frac{1}{2}(P+Q)$. For continuous fields, KL divergence becomes:

$$KL(P \parallel M) = \int_{\boldsymbol{T}} p(x) \log \frac{p(x)}{q(x)} dx \tag{10}$$

By calculating the $JSD(\boldsymbol{\phi}^+ \parallel \boldsymbol{\phi}^-)$ between the posterior and prior after each iteration, we can use it as a criterion for determining whether the model is stable.

5. SIMULATION RESULTS

To validate the proposed estimation framework and coverage strategy, we conduct MATLAB simulations in a $20m \times 20m$ 2-D mission space $\boldsymbol{T}$. A virtual density field is generated using a 2-D Gaussian function to simulate target distribution. The MRS is initially deployed in a $2m \times 2m$ area at the lower left corner, with randomly positioned rovers maintaining a minimum safety spacing of $0.4m$. The global map resolution is set to $0.5m$. During sampling, we set the observation error standard deviation $\sigma_n^2 = 0.02$ for the normalized density distribution. The initial resolution $a_m = 4m$ and its iteration parameter $\alpha = 0.73$. For the GP model, we set the constant value 0 to uniformly initialize its prior mean. We choose the classic Radial Basis Function (RBF) as its kernel function, which can be defined as

$$\mathcal{K}(X, X^*) = \sigma_f^2 \exp(-\frac{\left\|X - X^*\right\|^2}{2l^2}) \tag{11}$$

where σ_f and l are two hyperparameters of the kernel function. By maximizing the marginal log-likelihood method, the hyperparameters we adopt are $\{\sigma_f, l\} = \{0.25, 2.21\}$.

During coverage control, each rover moves with a $1m$ step size. The process terminates when the MRS's moving distance meets convergence criteria. Next, We evaluate the framework using the MRS consisting of 5 rovers. Define the true density distribution function as a 2-D Gaussian function model:

$$Z_r = A \cdot \exp[-z_a(x - z_x)^2 - z_b(y - z_y)^2] \tag{12}$$

where A represents the peak value of density distribution. z_a and z_b are the attenuation coefficients in the x and y directions respectively. $(z_x\ ,\ z_y)$ are the coordinates of the hotspot center of the density distribution, corresponding to the key area that needs to be monitored. Finally, the parameters $\{A, z_a, z_b, z_x, z_y\} = \{1, 0.05, 0.05, 0, 0\}$ are selected to generate the real density distribution, and its spatial shape is shown in Fig. 2a.

5.1 Regional division results

At this stage, 5 rovers are randomly deployed in the lower left starting area. Assume that the density function in space $\boldsymbol{T}$ at this time is a constant function $\mathbf{1}(q)$. Through the minimization calculation of the cost function $\boldsymbol{C}$ shown in (5), the optimized movement path of each rover is generated, as shown in Fig. 2b. In this stage, the moving distance of each rover is calculated, and the stability threshold $\Delta_{p_i} = 0.001m$ is set as the convergence criterion. When the displacement of all rovers is less than the threshold in 4 consecutive iterations, the system is judged to have reached a steady-state equilibrium.

5.2 Estimation results

Each rover fixes its own Voronoi region through region division, and estimates the unknown density online through sampling. Fig. 2c shows the moving trajectory of the rover during sampling. Fig. 3 shows each rover's estimated density field mapping, where jsd_s denotes JS divergence between its iterations and jsd_r between its estimate and true density. Through online updates and data fusion, all estimates asymptotically converge to the true field. Besides, Fig. 4a records the change process of jsd_r of each rover during the estimation process. Experimental results demonstrate that each rover's jsd_r exhibits a rapid initial decline followed by slower convergence. This two-stage characteristic ensures efficient estimation while progressively improving accuracy.

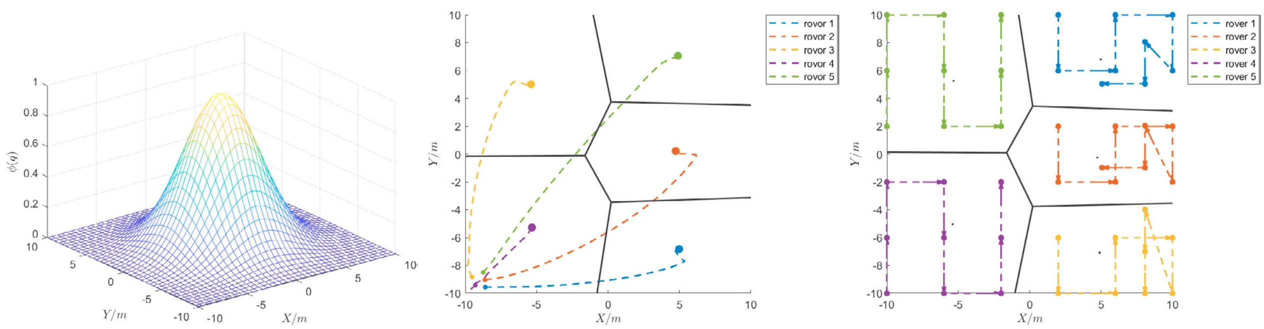

(a) Real density function (b) Region Division (c) Sampling trajectories

Fig. 2. (a): The demonstration of the real density function (b):The rovers move from the initial small point to the final large point. (c): The rovers move in the direction of the arrow. Rovers 4 and 5 have just completed the first round of sampling, while rovers 1, 2, and 3 have changed the sampling resolution α_m and started the second round.

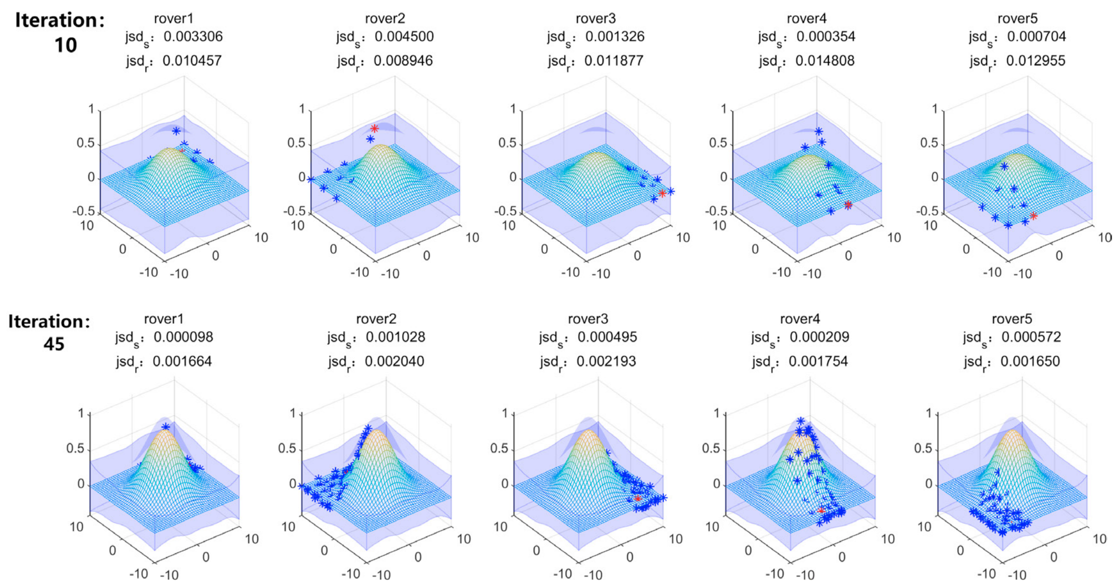

Fig. 3. Distributive and online estimation process. The surface represents the estimated density, with light blue area showing the 95% confidence interval. Blue and red points indicate historical and current sampling positions.

The framework uses JS divergence within and between rovers to determine convergence. the stable threshold of the estimation process is selected as $\{jsd_s, jsd_o\} = \{0.0004, 0.00065\}$. Where jsd_o reflects the JS divergence difference between rovers. The model is considered convergent when both JS divergence metrics remain below their thresholds for five consecutive iterations.

5.3 Optimal coverage results

Fig. 4b shows the MRS movement process based on Voronoi centroid coverage control after merging the estimated density sets. Each rover moves to the centroid of the Voronoi region weighted by density $\hat{\phi}(q)$ under this control. Set the stability threshold $\Delta p_i = 0.001$. The system reaches steady state when all rovers' movement distances are below this threshold for 4 consecutive iterations. Fig. 4c compares the cost function $\boldsymbol{C}$ changes with and without density weighting.

6. CONCLUSION

This paper proposes a coverage control method for MRS in unknown density field planetary, including a distributed and online density estimation and its coverage strategy. Firstly, a virtual uniform density field is adopted to uniformly cover the mission space for allocating each rover area. Secondly, based on reciprocating sampling, a distributed and online GP-regression method is used and combined with a multi-source fusion mechanism to form an estimated mapping of the unknown density field. The system stability is determined by its iterative JS divergence. Finally, the optimal coverage is achieved based on the estimated density. The simulation results demonstrate the effectiveness of the proposed framework, which has the advantage of requiring no prior assumptions about density and the complexity of the algorithm is only related to the map resolution, and has high environmental adaptability.

This study did not address rover coverage or map obstacles. Future work will explore coverage control with range limitations and obstacles, as well as 3D unknown space coverage for practical MRS applications.

ACKNOWLEDGEMENTS

This work was partly supported by the State Key Laboratory of Micro-Spacecraft Rapid Design and Intelligent

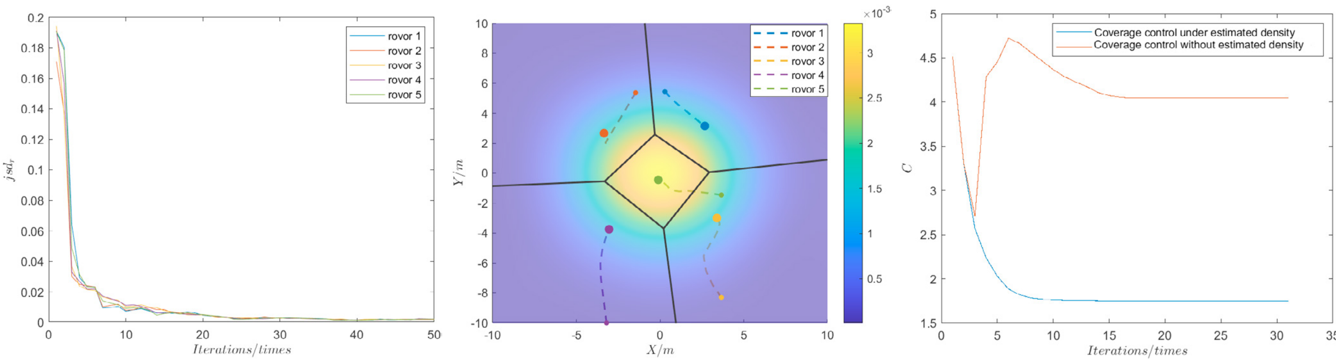

(a) The jsd_r value of each rover (b) Optimal coverage (c) Changes in the cost function

Fig. 4. (a): The jsd_r value of each rover reflects the deviation between distributions, with values closer to 0 indicating higher similarity. During coarse sampling, the system rapidly estimates regional density using a larger map resolution, causing jsd_r to decrease sharply with significant fluctuations. In the fine sampling stage, resolution is progressively reduced to improve estimation accuracy, while jsd_r fluctuations gradually converge. (b):Each rover moves from the position after sampling to the optimal coverage position, that is, from the small point to the large point. (c):Comparative analysis shows that the cost function shows a more significant decrease in the estimated density compared to the case where there is no estimated density weighting.

Cluster under grant No. MS01240110, the National Natural Science Foundation of China under grant No. 62303002, and the Key Program of Natural Science Foundation of Anhui Higher Education Institutions of China under grant No. 2022AH050068.

REFERENCES

Arum, S.C., Grace, D., and Mitchell, P.D. (2020). A review of wireless communication using high-altitude platforms for extended coverage and capacity. *Computer Communications*, 157, 232–256.

Carron, A., Todescato, M., Carli, R., Schenato, L., and Pillonetto, G. (2015). Multi-agents adaptive estimation and coverage control using gaussian regression. In *2015 European Control Conference (ECC)*, 2490–2495. IEEE.

Cortes, J., Martinez, S., Karatas, T., and Bullo, F. (2004). Coverage control for mobile sensing networks. *IEEE Transactions on robotics and Automation*, 20(2), 243–255.

Demetriou, M.A. and Hussein, I.I. (2009). Estimation of spatially distributed processes using mobile spatially distributed sensor network. *SIAM Journal on Control and Optimization*, 48(1), 266–291.

Dengyun, Y., Xueying, W., and Weiren, W. (2016). Review of technology development for chinese lunar exploration program. *Journal of Deep Space Exploration*, 3(4), 307–314.

Du, Q., Faber, V., and Gunzburger, M. (1999). Centroidal voronoi tessellations: Applications and algorithms. *SIAM review*, 41(4), 637–676.

Gong, W., Zhu, M., Zhang, Y., Chen, T., and Zheng, Z. (2024). Adaptive collaborative coverage control for multi-stratospheric airship within unknown nonuniform wind field. *Journal of the Franklin Institute*, 361(17), 107244.

Gu, J., Su, T., Wang, Q., Du, X., and Guizani, M. (2018). Multiple moving targets surveillance based on a cooperative network for multi-uav. *IEEE Communications Magazine*, 56(4), 82–89.

Kisantal, M., Sharma, S., Park, T.H., Izzo, D., Märtens, M., and D'Amico, S. (2020). Satellite pose estimation challenge: Dataset, competition design, and results. *IEEE Transactions on Aerospace and Electronic Systems*, 56(5), 4083–4098.

Popović, M., Vidal-Calleja, T., Hitz, G., Chung, J.J., Sa, I., Siegwart, R., and Nieto, J. (2020). An informative path planning framework for uav-based terrain monitoring. *Autonomous Robots*, 44(6), 889–911.

Reece, S. and Roberts, S. (2010). An introduction to gaussian processes for the kalman filter expert. In *2010 13th International Conference on Information Fusion*, 1–9. IEEE.

Schwager, M., Rus, D., and Slotine, J.J. (2009). Decentralized, adaptive coverage control for networked robots. *The International Journal of Robotics Research*, 28(3), 357–375.

Wang, J., Ju, C., Gao, Y., Kim, G.j., et al. (2018). A pso based energy efficient coverage control algorithm for wireless sensor networks. *Computers, Materials & Continua*, 56(3).

WANG, P., YU, X., and GUO, J. (2022). A survey of lunar wide range exploration rover and gnc technology. *Journal of Astronautics*, 43(5), 548.

Williams, C.K. and Rasmussen, C.E. (2006). *Gaussian processes for machine learning*, volume 2. MIT press Cambridge, MA.

Xu, A., Viriyasuthee, C., and Rekleitis, I. (2011). Optimal complete terrain coverage using an unmanned aerial vehicle. In *2011 IEEE International conference on robotics and automation*, 2513–2519. IEEE.

Yu, D., Xu, H., Chen, C.P., Bai, W., and Wang, Z. (2021). Dynamic coverage control based on k-means. *IEEE Transactions on Industrial Electronics*, 69(5), 5333–5341.

Zhang, L., Zhang, Z., Siegwart, R., and Chung, J.J. (2021). Distributed pdop coverage control: Providing large-scale positioning service using a multi-robot system. *IEEE Robotics and Automation Letters*, 6(2), 2217–2224.

Zhong, M. and Cassandras, C.G. (2011). Distributed coverage control and data collection with mobile sensor networks. *IEEE Transactions on Automatic Control*, 56(10), 2445–2455.